CHINESE JOURNAL OF MECHANICAL ENGINEERING
Vol. 27, No. 5, 2014

DOI: 10.3901/CJME.2014.0723.125, available online at www.springerlink.com; www.cjmenet.com; www.cjmenet.com.cn

A Comparison in Laser Precision Drilling of Stainless Steel 304 with Nanosecond and Picosecond Laser Pulses

ZHANG Hongyu[1], DI Jianke[2], ZHOU Ming[1, *], and YAN Yu[3]

1 *State Key Laboratory of Tribology, Tsinghua University, Beijing 100084, China*
2 *Center for Photon Manufacturing Science and Technology, Jiangsu University, Zhenjiang 212013, China*
3 *Corrosion and Protection Center, Beijing University of Science and Technology, Beijing 100083, China*

Received July 24, 2013; revised March 11, 2014; accepted July 23, 2014

Abstract: Precision drilling with picosecond laser has been advocated to significantly improve the quality of micro-holes with reduced recast layer thickness and almost no heat affected zone. However, a detailed comparison between nanosecond and picosecond laser drilling techniques has rarely been reported in previous research. In the present study, a series of micro-holes are manufactured on stainless steel 304 using a nanosecond and a picosecond laser drilling system, respectively. The quality of the micro-holes, e.g., recast layer, micro-crack, circularity, and conicity, etc, is evaluated by employing an optical microscope, an optical interferometer, and a scanning electron microscope. Additionally, the micro-structure of the samples between the edges of the micro-holes and the parent material is compared following etching treatment. The researching results show that a great amount of spattering material accumulated at the entrance ends of the nanosecond laser drilled micro-holes. The formation of a recast layer with a thickness of ~25 μm is detected on the side walls, associated with initiation of micro-cracks. Tapering phenomenon is also observed and the circularity of the micro-holes is rather poor. With regard to the micro-holes drilled by picosecond laser, the entrance ends, the exit ends, and the side walls are quite smooth without accumulation of spattering material, formation of recast layer and micro-cracks. The circularity of the micro-holes is fairly good without observation of tapering phenomenon. Furthermore, there is no obvious difference as for the micro-structure between the edges of the micro-holes and the parent material. This study proposes a picosecond laser helical drilling technique which can be used for effective manufacturing of high quality micro-holes.

Keywords: laser drilling, nanosecond laser, picosecond laser, helical drilling, recast layer

1 Introduction

Nowadays, the increasing demand in manufacturing of micro-features in semiconductor, ceramic, and metal materials has promoted the application of laser precision drilling in aerospace, automotive, and medical industries[1]. Specifically, as a versatile and reliable technique, laser drilling has been used to manufacture shaped film holes, i.e., micro-holes with irregular shapes or inclined directions, which form a protective cooling layer between the external surfaces of the engine components (e.g., turbine blade, and combustion chamber, etc) and the hot gases[2]. In general, lasers with short pulses (e.g., millisecond and nanosecond) are of industrial relevance with an acceptable compromise between accuracy and efficiency[3–4]. However, when using these lasers, the molten material would re-solidify and accumulate on the side wall of the micro-hole, resulting in the formation of a recast layer and thermal damage to the workpiece[5]. These issues have caused much attention because the recast layer is considered to be extremely detrimental as the potential sites for the generation of micro-cracks, which, in addition to other defects such as spattering and tapering, has limited application of laser drilling in the situations where precision micro-holes with high quality are required[6].

Consequently, different strategies have been attempted to further improve the quality of the micro-holes, e.g., introduction of ultrasonic vibration[7] and underwater working environment[8]. In particular, it has been suggested that a reduction in pulse duration down to picosecond and femtosecond scale may probably overcome the thermally induced issues[9–10]. However, although femtosecond laser ablation has been advocated as an appropriate method of choice owing to removal of materials through vaporization[11], the requirement in demanding maintenance and the complexity in optical devices make it difficult for industrial applications. In addition, it is pointed out by Dausinger et al. that when the pulse duration is below 10 ps, a further reduction will produce no remarkable advantage for material removal, at least for metals[12]. Considering the

* Corresponding author. E-mail: zhouming@tsinghua.edu.cn
Supported by National Basic Research Program of China (Grant No. 2011CB013004), National Natural Science Foundation of China (Grant No. 51005130), and Research Fund of State Key Laboratory of Tribology, Tsinghua University (Grant no. SKLT12B06)

nonlinear interaction mechanism during femtosecond laser ablation, it is recommended that a pulse duration of 5–10 ps may be optimal for laser micro-machining[13]. Therefore, precision drilling with picosecond laser is regarded as a better alternative on condition that the laser parameters, such as average power, repetition rate, and focal position etc, are properly adjusted[14].

Although there are an amount of studies in literature to investigate laser drilling techniques, it is considered that a detailed comparison as to the quality of micro-holes drilled with nanosecond and picosecond lasers has been lacking. Consequently, in the present study we primarily aim to gain an insight into this issue, focusing on surface morphology and formation of recast layer etc during nanosecond and picosecond laser drilling of through micro-holes.

2 Materials and Methods

2.1 Nanosecond and picosecond laser drilling system

The laser drilling experiments were performed on the workpiece of stainless steel 304 with a thickness of 1.0 mm using a nanosecond and a picosecond laser drilling system, respectively.

The schematic diagram of the nanosecond laser drilling system is shown in Fig. 1, which incorporates an Nd:YVO4 laser and a series of optical components into a precision platform. In detail, the laser beam firstly passes through a quarter-wave plate to enable circular polarization, and then through a beam expander before it is reflected by a mirror. Subsequently, the laser beam is guided by a high speed scanner and a field lens to achieve accurate scanning over the workpiece with adjustable laser focal position. The workpiece is fixed tightly on the precision platform using a clamping device. In addition, an integrated gas blowing and dust collecting apparatus is established to facilitate removal of materials.

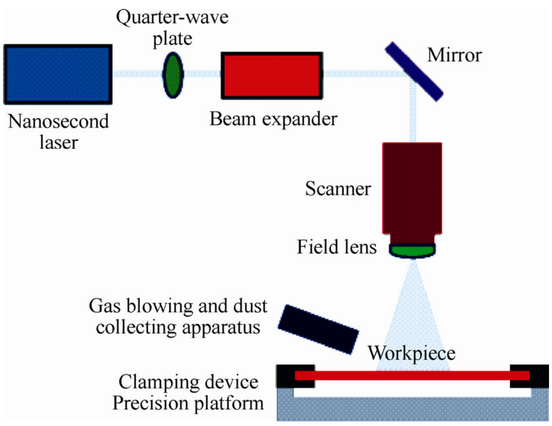

Fig. 1. Schematic diagram of the nanosecond laser drilling system

The schematic diagram of the picosecond laser drilling system is shown in Fig. 2, which combines a Lumera laser, a high-speed laser beam-rotation apparatus (~2000 r/min), and several optical components with an Aerotech five-axis positioning platform. Specifically, the laser beam is focused on the workpiece by a focusing lens after being reflected by a mirror and passing through the beam-rotation apparatus. The focusing lens is equipped onto a vertical adjustment device, through which the height of the laser focal position can be changed simultaneously with removal of materials. Therefore, the focal spot is always maintained on the top surface of the workpiece, which is fixated on the Aerotech positioning platform. A helical path of the laser beam relative to the workpiece is achieved through synergistic functioning of vertical adjustment in the focal position of the laser beam and horizontal movement of the workpiece. Furthermore, a co-axial gas nozzle is integrated into the drilling system to provide nitrogen as the assist gas.

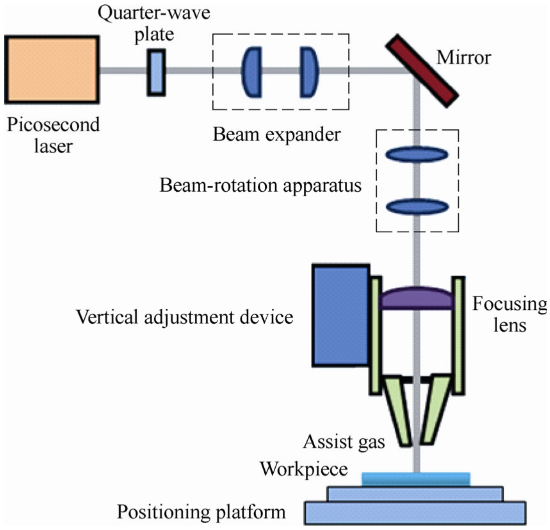

Fig. 2. Schematic diagram of the picosecond laser drilling system

2.2 Experimental setup

Trepanning drilling was performed using the Nd:YVO4 nanosecond laser at a wavelength of 532 nm and a pulse duration of 12 ns, with the average power and the repetition rate set at 30 W and 100 kHz, respectively. A series of micro-holes with a diameter of 0.5 mm (shown as H_1–H_8) were manufactured at different moving speeds of the laser beam ranging from 100 mm/s to 2000 mm/s. In addition, helical drilling was conducted employing the Lumera picosecond laser at a wavelength of 1064 nm and a pulse duration of 10 ps. The primary parameter setup included average power, repetition rate, assist gas pressure, speed of the positioning platform etc. A cavalcade of micro-holes with different diameters ranging from 0.2 mm to 0.6 mm was manufactured. The nanosecond and picosecond laser drilling parameters were shown in detail in Table 1.

Unless otherwise mentioned, all the micro-holes were drilled vertically at 90° to the workpiece, with the laser beam focusing on the top surface of the workpiece. In addition, manufacturing of each hole was repeated at least four times to enable statistical relevance.

Table 1. Nanosecond and picosecond laser precision drilling parameters

Parameter setup	Nanosecond laser drilling	Picosecond laser drilling
Average power P/W	30	6.5
Repetition rate F/kHz	100	80
Laser beam moving speed $V_{\mathrm{lb}}/10^2(\mathrm{mm}\cdot\mathrm{s}^{-1})$	H_1: 1; H_2: 3; H_3: 5; H_4: 7 H_5: 9; H_6: 11; H_7: 15; H_8: 20	—
Assist gas pressure N/MPa	0.4	0.64
Positioning platform speed $V_{\mathrm{pp}}/(\mathrm{mm}\cdot\mathrm{s}^{-1})$	—	0.5

2.3 Characterization of laser drilled micro-holes

Following nanosecond and picosecond laser drilling, the micro-holes were initially examined utilizing a Quanta 200 FEG scanning electron microscope (SEM, FEI, Netherlands) to detect spattering and formation of recast layer without any treatment of the samples. Additionally, the micro-holes were evaluated using a microXAM optical interferometer (KLA-Tencor, USA) in order to obtain three-dimensional (3D) surface topography. Subsequently, the entrance ends of the micro-holes were polished by polyurethane polishing pad with the presence of slurry, and further investigated by the SEM associated with an energy dispersive X-ray (EDX) analysis to facilitate comparison of elemental composition between the edges of micro-holes and the parent material. Furthermore, the samples were etched using aqua regia, and the micro-structure was examined by a BX60M optical microscope (Olympus, Japan) and the SEM in order to reveal the recast layer more clearly.

3 Results and Discussion

3.1 Nanosecond laser drilled holes

It was demonstrated from the SEM micrographs in Fig. 3 that, for the micro-holes drilled by nanosecond laser, there was a great amount of spattering material accumulating at the entrance end, and formation of a recast layer (average thickness: ~20 μm) on the side wall was detected following slight polishing process. In order to view the quality of the micro-holes more obviously, the surface with the entrance end was further polished and examined by the SEM, Fig. 4. It was clearly shown from this figure that the conicity of the micro-holes was becoming more and more distinctive from H_1 to H_8, with the increase of the laser beam moving speed. For example, the diameter of the micro-hole H_8 was only about 35 μm at the exit end. In addition, the circularity of the micro-holes seemed to be getting worse as well, and the presence of ripple-like morphology was observed on the side walls of the micro-holes, e.g., H_4 to H_8, indicating an incomplete removal of materials. From the enlarged SEM micrographs of the micro-holes from H_2 to H_5 as shown in Fig. 5, the formation of recast layer and micro-cracks on the side walls could be clearly detected.

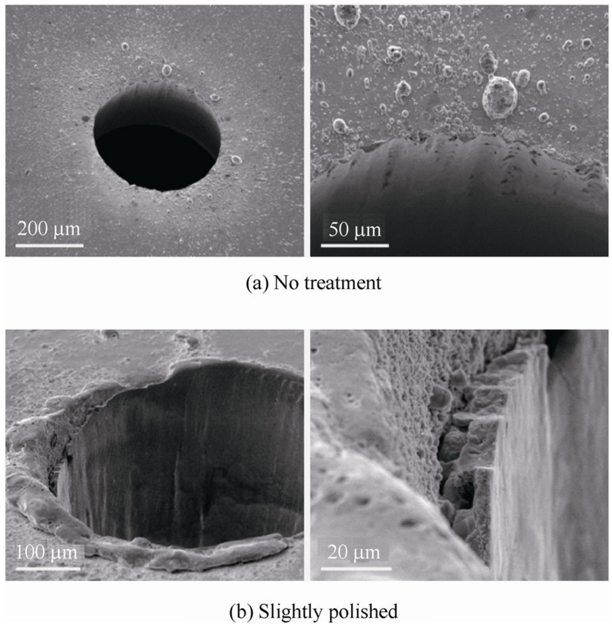

Fig. 3. Entrance ends of the micro-holes manufactured with nanosecond laser drilling

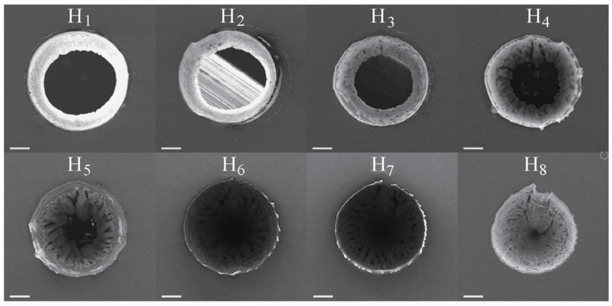

Fig. 4. SEM micrographs of deterioration of conicity and circularity for the micro-holes from H_1 to H_8, bar length: 100 μm

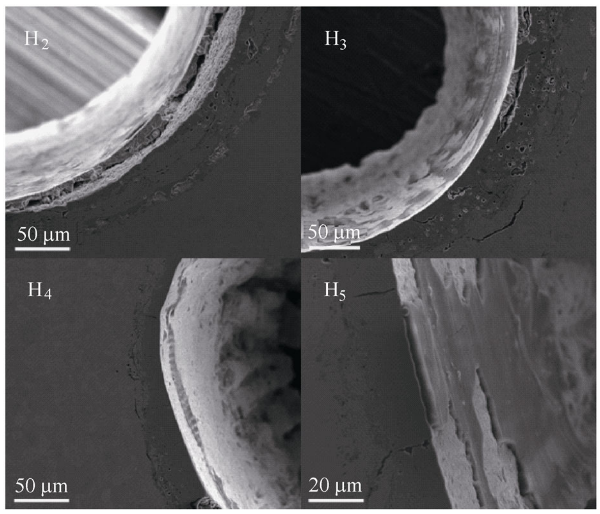

Fig. 5. Enlarged SEM micrographs of the presence of recast layer and micro-cracks on the side walls of the micro-holes

Comparison of elemental composition between the edges of the micro-holes (position 1) and the parent material (position 2) was shown in Fig. 6 and Table 2, from which it was indicated that the content of oxygen was greatly higher at the edges of the micro-holes. This could be attributed to the introduction of oxygen in the air to the molten material before it re-solidified on the side walls and formed the recast layer. Furthermore, the presence of recast layer and micro-cracks could be validated through comparison of the micro-structure of the samples following etching treatment, as indicated from the SEM micrographs in Fig. 7.

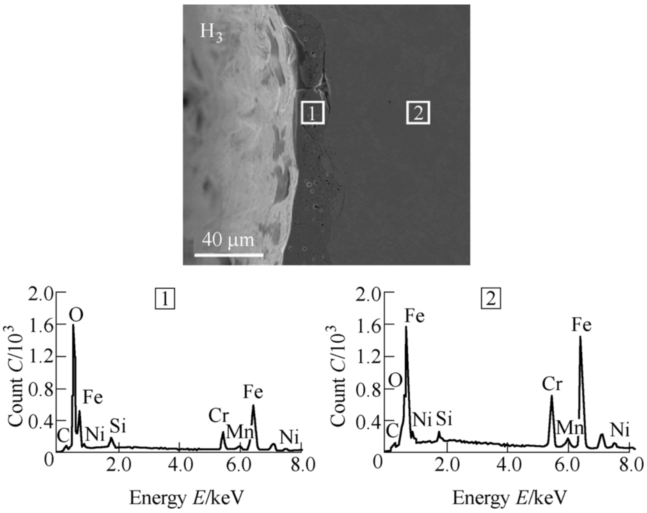

Fig. 6. Elemental composition comparison between the edges of the micro-holes (position 1) and the parent material (position 2)

Table 2. Element composition between edges of nanosecond laser drilled holes and parent material wt%

Element	Fe	Cr	Ni	Mn	Si	C	O
Micro-hole edge	63.2	12.8	6.3	1.6	1.4	0.6	14.1
Parent material	71.9	17.4	6.1	1.4	0.9	0.6	1.7

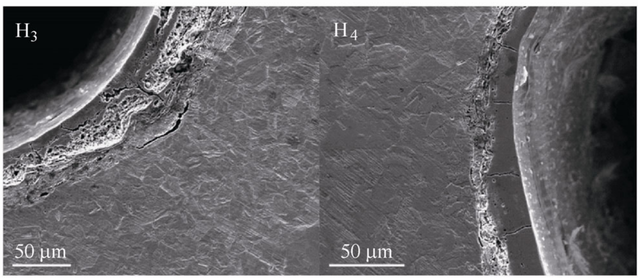

Fig. 7. SEM micrographs of micro-structure of the samples following etching treatment

3.2 Picosecond laser drilled holes

The SEM micrographs in Fig. 8 demonstrated the surface morphology of both the entrance ends and the exit ends of the micro-holes drilled using picosecond laser. Although it appeared rougher with regard to the entrance ends because this surface of the original samples was not polished prior to laser drilling, it was obvious from these images that both ends were absent from accumulation of spattering material. However, the presence of a very tiny amount of residual metal flakes with a height of ~5 μm at the entrance ends of the micro-holes could be observed, as shown from the 3D optical interferometric micrographs and also the 2D surface profiles of the micro-holes, Figs. 9 and 10.

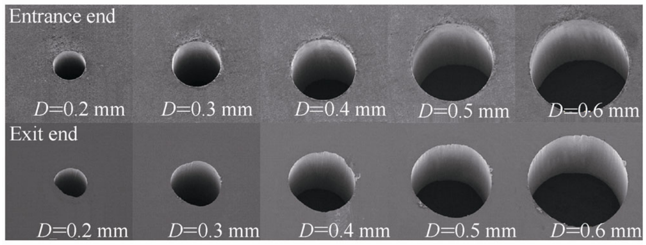

Fig. 8. SEM micrographs of the entrance ends and the exit ends of the micro-holes prepared by picosecond laser drilling

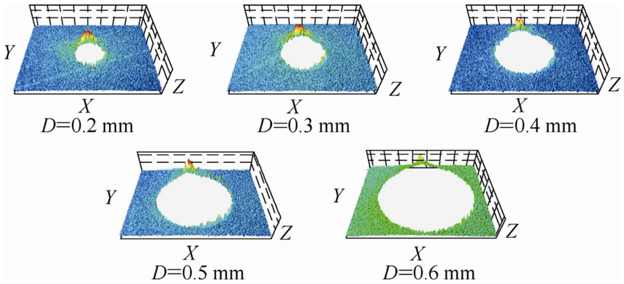

Fig. 9. 3D surface topography of the entrance ends of the micro-holes with the presence of residual metal flakes, scale: X (0.8 mm), Y (0.6 mm), Z (4 μm)

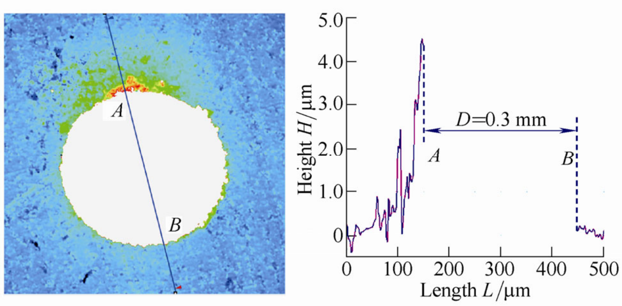

Fig. 10. 2D surface profile of the entrance end of the micro-hole (diameter: 0.3 mm) with the height of residual metal flakes

The residual metal flakes were easily removed by slight polishing, and the SEM micrographs of the entrance ends after polishing were shown in Fig. 11. It was obvious that the circularity of the micro-holes was fairly good without the occurrence of tapering phenomenon. In addition, the enlarged SEM micrographs in Fig. 12 indicated a whitish zone (width: ~5 μm) along the perimeter of the micro-holes, which might be the recast layer re-solidifying on the side walls. However, the difference in elemental composition between this whitish zone and the parent material was not significant, Table 3. As a consequence, it was considered that the formation of this whitish zone could be attributed to the accumulation of secondary electrons at the edges of the micro-holes, resulting in an inauthentic discrepancy in the brightness of the image. This speculation was further confirmed through the optical and SEM micrographs of the samples following etching treatment, as the micro-structure between the whitish zone and the parent material was almost the same, which were typically characterized by the presence of austenite grain and twin crystal, Fig. 13.

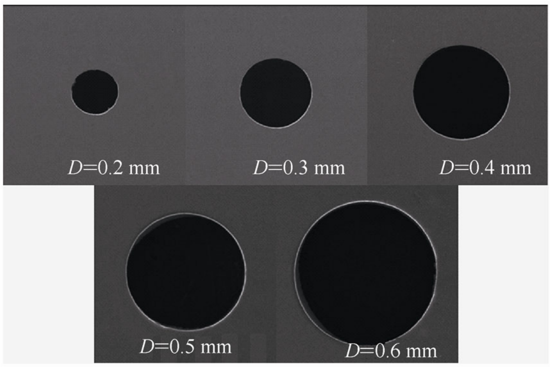

Fig. 11. SEM micrographs of the entrance ends of the micro-holes after slight polishing

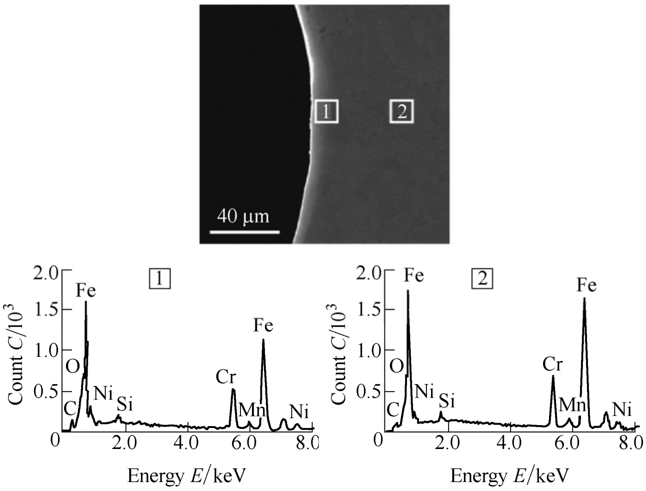

Fig. 12. Elemental composition comparison between the edges of the micro-holes (position 1) and the parent material (position 2)

Table 3. Element composition between edges of picosecond laser drilled holes and parent material wt%

Element	Fe	Cr	Ni	Mn	Si	C	O
Micro-hole edge	71.9	17.7	6.1	1.8	0.6	0.6	1.3
Parent material	72.2	17.5	6.1	1.5	0.7	0.4	1.6

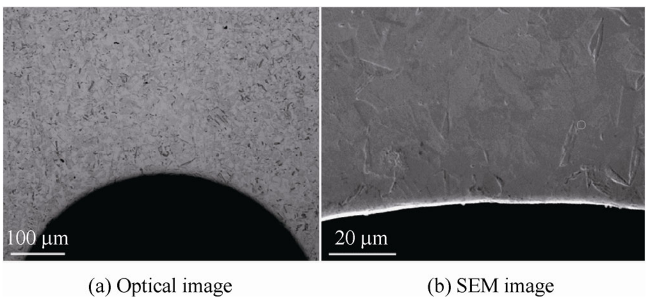

(a) Optical image (b) SEM image

Fig. 13. Optical and SEM micrographs of micro-structure of the samples following etching treatment

3.3 Influence of laser drilling parameters on the quality of the micro-holes

In the present study, the quality of the micro-holes manufactured by nanosecond and picosecond laser drilling was comprehensively evaluated. It was demonstrated from the SEM and 3D interferometric micrographs that the picosecond laser drilled micro-holes were quite smooth and the recast layer was greatly reduced without the formation of micro-cracks. The achievement of such high quality micro-holes can be attributed to the optimal parameter setup as shown in Table 1, in addition to the application of the helical drilling strategy.

The determination of the drilling parameters was based on a series of pre-tests and previously published studies[15–16], in which the influence of various laser parameters on the formation of recast layer was extensively investigated. In the present study, a major improvement is that the laser beam is always focused on the top surface of the samples through the use of a vertical adjustment device. Therefore, the minimum focal spot size can be maintained in order to ensure the maximum attainable energy intensity during laser drilling. This is considered to be beneficial for the removal of materials. In addition, another important difference associated with the current picosecond laser drilling system is the introduction of the beam-rotation apparatus, through which a high-speed rotation of the laser beam can be steadily achieved. Ideally, the laser intensity is spatially distributed in a Gaussian form within the laser spot, and the rotation of the laser beam can effectively eliminate the influence of the distortion in practice and correspondingly further reshape the holes with a greatly increased efficiency. Furthermore, the application of helical drilling also contributes to reduction of the recast layer and improvement in geometrical accuracy of the micro-holes, as in this process the material can be removed laterally and does not need to be expelled axially along the side wall of the hole to the entrance end[17].

In spite of the high quality of micro-holes manufactured with picosecond laser drilling, it should be noted that the circularity of the micro-holes at the exit ends is not very good, especially for the micro-holes with smaller diameter. Further research is required to establish the optimal drilling parameters to overcome this issue, e.g., increasing the laser average power, etc.

3.4 Material removal mechanism during nanosecond and picosecond laser drilling

In comparison with nanosecond laser drilling, the great improvement in the quality of micro-holes manufactured with picosecond laser drilling indicated that the material removal mechanism was completely different when using these two lasers.

With regard to nanosecond laser, the laser beam-matter interaction mode is dominated by heat conduction, and the material is removed mainly through melting, with partial evaporation and plasma formation[18–19]. However, the molten material will re-solidify and accumulate on the side wall of the micro-hole if it is not expelled completely and rapidly, designated as the recast layer.

As for picosecond laser, the thermal behaviour between laser beam and matter abides by the two-temperature model[20]. Following a multi-photon absorption process, the electrons re-establish the Fermi distribution within a few femtoseconds and then transfer the energy to the lattice, with a typical electron-phonon relaxation time on the order of tens of picoseconds. As this relaxation time is similar to laser pulse duration, it can not be negligible. Consequently, the electron temperature is much higher than that of the lattice, characterized by a non-equilibrium energy transport mechanism[21]. As a result, the removal of materials by picosecond laser is mainly through direct evaporation with a tiny amount of melting. Therefore, formation of recast layer and thermal damage to the workpiece can be greatly reduced.

4 Conclusions

(1) The micro-holes manufactured by nanosecond laser drilling are characterized by the presence of an amount of spattering material at the entrance ends and the formation of recast layer and micro-cracks on the side walls. Conicity and circularity of the micro-holes are also poor.

(2) The entrance ends, exits ends, and the side walls of the micro-holes prepared by picosecond laser drilling are smooth, without accumulation of spattering material, and formation of recast layer and micro-cracks. The circularity is fairly good with no detection of tapering phenomenon.

(3) The material removal mechanism for nanosecond and picosecond laser drilling is completely different, with the former mainly dominated by thermally induced melting and the latter through direct evaporation.

(4) Picosecond laser helical drilling could be widely used in various industrial applications for the manufacturing of high quality micro-holes in the future.

References

[1] ZUO Tiechuan, CHEN Hong. Green manufacture in 21 century: laser manufacturing technology and application[J]. *Chinese Journal Mechanical Engineering*, 2009, 45(10): 106–110. (in Chinese)

[2] BUNKER R S. A review of shaped hole turbine film cooling technology[J]. *J Heat Trans-T ASME*, 2005, 127(4): 441–453.

[3] LEIGH S, SEZER K, LI L, et al. Recast and oxide formation in laser-drilled acute holes in CMSX-4 nickel single-crystal superalloy[J]. *Proc IMechE-Part B: J Engineering Manufacture*, 2010, 224(B7): 1005–1016.

[4] ZHANG Yongkang, ZHANG Lei, LUO Kaiyu, et al. Effects of laser shock processing on mechanical properties of laser welded ANSI 304 stainless steel joint[J]. *Chinese Journal Mechanical Engineering*, 2012, 25(2): 285–292.

[5] SEZER H K, LI L, SCHMIDT M, et al. Effect of beam angle on HAZ, recast and oxide layer characteristics in laser drilling of TBC nickel superalloys[J]. *Int. J. Mach. Tool Manu.*, 2006, 46(15): 1972–1982.

[6] BANDYOPADHYAY S, SARIN-SUNDAR J K, SUNDARARAJAN G, et al. Geometrical features and metallurgical characteristics of Nd:YAG laser drilled holes in thick IN718 and Ti-6Al-4V sheets[J]. *J. Mater. Process Technol.*, 2002, 127(1): 83–95.

[7] KANG B, KIM G W, YANG M Y, et al. A study on the effect of ultrasonic vibration in nanosecond laser machining[J]. *Opt. Laser Eng.*, 2012, 50(12): 1817–1822.

[8] ZHANG Hua, XU Jiawen, ZHAO Jianshe, et al. Mechanism of recast removal during laser drilling underwater[J]. *Adv. Sci. Lett.*, 2011, 4(6–7): 2071–2075.

[9] HU W Q, SHIN Y C, KING G B. Micromachining of metals, alloys, and ceramics by picosecond laser ablation[J]. *J. Manuf. Sci. E-T ASME*, 2010, 132(1): 1–7.

[10] ZHAO Qingliang, JIANG Tao, DONG Zhiwei, et al. Ablation threshold and material removal mechanisms of SiC processed by femtosecond laser[J]. *Chinese Journal Mechanical Engineering*, 2010, 46(21): 172–177. (in Chinese)

[11] KAMLAGE G, BAUER T, OSTENDORF A, et al. Deep drilling of metals by femtosecond laser pulses[J]. *Appl. Phys. A*, 2003, 77(2): 307–310.

[12] DAUSINGER F, HUGEL H, KONOV V. Micro-machining with ultrashort laser pulses: from basic understanding to technical applications[J]. *Proc. SPIE*, 2003, 5147: 106–115.

[13] FOHL C, BREITLING D, DAUSINGER F. Precise drilling of steel with ultrashort pulsed solid-state lasers[J]. *Proc. SPIE*, 2003, 5121: 271–279.

[14] ANCONA A, NODOP D, LIMPERT J, et al. Microdrilling of metals with an inexpensive and compact ultra-short-pulse fiber amplified microchip laser[J]. *Appl. Phys. A*, 2009, 94(1): 19–24.

[15] LOW D K Y, LI L, CORFE A G. Characteristics of spatter formation under the effects of different laser parameters during laser drilling[J]. *J. Mater. Process Technol.*, 2001, 118(1): 179–186.

[16] CHIEN W T, HOU S C. Investigating the recast layer formed during the laser trepan drilling of Inconel 718 using the Taguchi method[J]. *Int. J. Adv. Manuf. Technol.*, 2007, 33(3–4): 308–316.

[17] KASPAR J, LUFT A, NOLTE S, et al. Laser helical drilling of silicon wafers with ns to fs pulses: Scanning electron microscopy and transmission electron microscopy characterization of drilled through-holes[J]. *J. Laser Appl.*, 2006, 18(2): 85–92.

[18] LEITZ K H, REDLINGSHOFER B, REG Y, et al. Metal ablation with short and ultrashort laser pulses[J]. *Physics Procedia*, 2011, 12(Part B): 230–238.

[19] LEITZ K H, KOCH H, OTTO A, et al. Numerical simulation of process dynamics during laser beam drilling with short pulses[J]. *Appl. Phys. A*, 2012, 106(4): 885–891.

[20] CHICHKOV B N, MOMMA C, NOLTE S, et al. Femtosecond, picosecond and nanosecond laser ablation of solids[J]. *Appl. Phys. A*, 1996, 63(2): 109–115.

[21] JIANG L, TSAI H L. Improve two-temperature model and its application in ultrashort laser heating of metal films[J]. *J. Heat Trans-T ASME*, 2005, 127(10): 1167–1173.

Biographical notes

ZHANG Hongyu, born in 1982, is currently a lecturer at *State Key Laboratory of Tribology, Tsinghua University, China*. He received his PhD degree from *University of Huddersfield, UK*, in 2009. His research interests include biotribology and laser manufacturing.
Tel: +86-10-62773129; E-mail: zhanghyu@tsinghua.edu.cn

DI Jianke, born in 1983, is currently a PhD candidate at *Center for Photon Manufacturing Science and Technology, Jiangsu University, China*.
E-mail: dijianke@hotmail.com

ZHOU Ming, born in 1972, is currently a professor at *State Key Laboratory of Tribology, Tsinghua University, China*. He received his PhD degree from *Jiangsu University, China*, in 2003. His research interests include laser manufacturing, bionic manufacturing, and biotribology.
Tel: +86-10-62783968; E-mail: zhouming@tsinghua.edu.cn

YAN Yu, born in 1980, is currently an associate professor at *Corrosion and Protection Center, Beijing University of Science and Technology, China*. He received his PhD degree from *Leeds University, UK*, in 2008. His research interest is biotribocorrosion.
Tel: +86-10-62332345; E-mail: yanyu@ustb.edu.cn